VOL. 10, NO. 16, SEPTEMBER 2015 ISSN 1819-6608
ARPN Journal of Engineering and Applied Sciences

www.arpnjournals.com

FUEL QUALIFICATION USING QUARTZ SENSORS

Muhammad Rivai and Tasripan
Department of Electrical Engineering, Institut Teknologi Sepuluh Nopember, Surabaya, Indonesia
E-Mail: muhammad_rivai@ee.its.ac.id

ABSTRACT

An array of quartz crystal sensors modified by chemical materials was implemented for vapor detection. In this study, the vapor sensor array was employed to qualify the fuels. This was done to distinguish some common fuels and also to determine the rate of fuel adulteration. All the measurements were conducted at room temperature. The sensor response consumed only up to one minute for a measurement cycle. After statistical data analysis including Principal Component Analysis and Neural Network methods, it was possible to conclude that the sensor array is able to distinguish the fuel vapors with high reproducibility and to determine the rate of fuel adulteration with linear correlation.

Keywords: fuel vapor, neural network, principal component analysis, quartz sensor array.

INTRODUCTION

Transportation plays a vital role in modern life. The flexibility and freedom to cover short and long distances increase the personal development and professional activities allowing better interaction among people. Unfortunately, transportation - particularly road transport -was indicated as an important contributor for air pollution associated with the hazards to the environment and human health [1]-[4]. Air toxic emissions of primary concern are benzene and polyaromatic hydrocarbons. Both have been identified as carcinogenic and mutagenic. Air toxic emissions such as benzene depend mainly on fuel composition and catalyst performance [5]. The fuels produced by the refineries usually comply with the existing specifications defined by government regulation to meet demand requirement and environmental considerations. However, changes in the fuel properties may occur through the shipping products via barges, tank truck or pipelines until the station storage tank which can result in contamination (e.g., water, tank sludge and residues) or adulteration with lower-priced materials (e.g., kerosene, marine diesel, recycled lubricants or industrial solvents). The adulterated fuels can increase nitrogen oxide, particulate matter and unburned hydrocarbon emissions [5], [6]. Kerosene is more difficult to ignite than gasoline, so its addition can increase the tailpipe emissions of hydrocarbons, carbon monoxide and particulate matter emissions [7].

The most common methods to estimate fuel composition qualitatively and quantitatively are gas chromatography and liquid chromatography [8]-[10]. These techniques involve the separation of mixtures of compounds by passing through a partition column. The differential partitioning into the stationary phase allows the compounds to be separated in time and space. Infrared and Fourier transform near infrared spectroscopes have been reported for quantitative analysis of volatile organic compound contained in fuels [9], [11], [12]. These methods are powerful tools for detecting hydrocarbon-based adulterants but require experienced and skilled professionals, costly equipments, and are time consuming. Therefore, an electronic nose device that is relatively simple, cheap and fast to determine the quality of fuels is of prime importance.

The electronic nose technology based device is designed to detect and identify among complex vapor mixtures using a sensor array. The sensor array is composed of a number of non-specific sensors with slightly different or overlapping response to each other. A vapor will stimulate sensor array to produce a fingerprint or pattern. The patterns from known vapors are used as references of a classifier so that unknown vapors can be recognized. The ranges of transduction mechanisms used in the electronic nose technology are metal-oxide semiconductor [13]-[19], conducting polymer sensors [20]-[22], surface acoustic wave [23]-[26], and quartz crystal microbalance [27]-[30]. In this paper, we use quartz crystal sensors coated with different chemical sensing materials to evaluate fuel qualification. Addition or subtraction of material on the surface of a quartz crystal, results in a change in its resonant frequency.

The excessive amounts of coating material on the crystal surface will reduce its quality factor, due to the acoustic losses, which cause the crystal to cease the oscillating mechanism. The sensing material film can bind the molecules of the vapor of interest decreasing the resonant frequency (f) of the device in proportion to the added mass (Δm). The shift frequency (Δf) is expressed by

$$\Delta f = -\frac{2f^2 \Delta m}{\rho v A} \quad (1)$$

where, ρ is the density of quartz (2.648 g/cm^3), v is the transverse wave velocity in quartz (3.336 x 10^5 cm/s), and A is the area of the quartz crystal. For a quartz crystal with a resonant oscillation frequency of 20 MHz, an addition of 1 μg of mass over an area of 1 cm^2 of the quartz crystal surface will result 905.6 Hz decrease in the oscillation frequency.

MATERIAL AND METHOD

The piezoelectric quartz crystals used in this study were AT-Cut 20-MHz with gold plated electrodes on both sides mounted in a HC-49/U crystal holder. The both sides of the crystal surfaces were coated with the chemically sensitive materials with different polarity: silicone OV-101 (non polar), OV-17 (mid polar) and polyethylene glycol PEG-6000 (polar) using ultrasonic atomizer method. The materials were dissolved in chloroform in a concentration of 1 mg/ml for their deposition on crystal electrodes. The 1.5 ml of film solution was contained in a flask located straight over the atomizer in order to allow the ultrasonic radiation to reach it. The frequency shift was monitored by a network analyzer and the deposition process would be stopped after reaching up to 20 KHz. The size of the produced mist particles is determined by the vibration frequency of the ultrasonic oscillator. In the case of 3.4 MHz-ultrasonic atomizer, the average size of the generated particles is about 3 μm [31].

Figure-1 depicts a schematic of the experimental set-up. The vapor generation system consisted of a 1 cubic meter of reference gas, 0.5 ml of liquid sample and a 12 volt three-way solenoid valve. The reference gas stream module was dry ultra high purity nitrogen, flowing at 100 ml/min that served to establish the baseline response and the vapor carrier. The sensor array was installed in a 1.2 ml sensor chamber and each sensor was connected to an oscillator circuit.

The sensor oscillators and a 20 MHz sealed quartz crystal as reference oscillator were fed to a binary subtracting circuit to provide a low frequency shift. The frequency shifts were then converted to voltage mode by a Frequency to Voltage (F-V) Converter with the sensitivity of 2.5 x 10^{-5} V/Hz and the signals were then amplified by an instrumentation amplifier with a gain of 210.

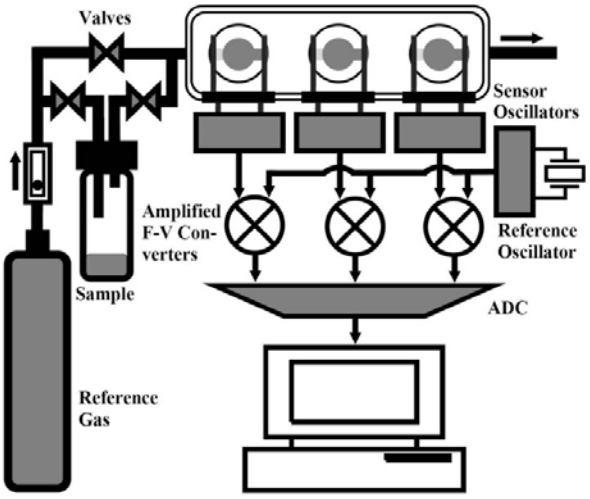

Figure-1. The schematic of the measurement system.

To keep output voltage remains unsaturated, the amplifier is equipped with dc offset to adjust the zero output as the sensor array responses to reference gas. Every 0.1 second, each frequency shift represented in voltage mode was then converted to digital information by 12-bit Analog to Digital Conversion (ADC) connected to a personal computer via Universal Serial Bus communication.

The measurements were performed at the temperature of 32.9 ± 1.5°C. The resonant frequency shift of the sensor was monitored before and after exposure to the sample vapors. The apparatus is used to detect and identify several fuel vapors having various physical and chemical properties including its adulteration. All of the samples including kerosene, diesel fuel, Pertamina Premium gasoline (octane number of 88), Pertamina Pertamax gasoline (octane number of 92), crude oil, and spiritus fuel were tested with gas chromatography method to obtain their compositions and properties. Principal Component Analysis (PCA) and neural network methods were employed to describe the discrimination rate.

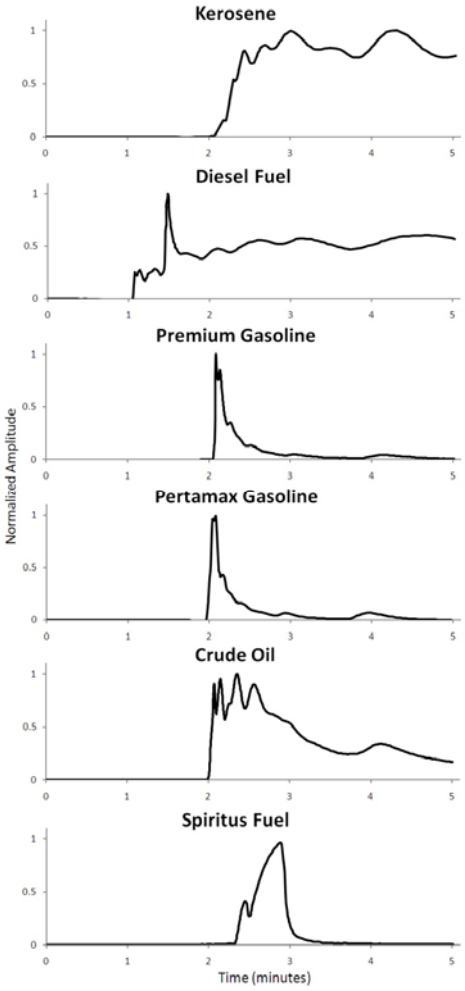

Figure-2. The chromatogram of the fuel samples.

RESULT AND DISCUSSIONS

Figure-2 shows the chromatograms of the fuel samples achieved on 45 m length x 0.25 mm internal diameter x 0.20 um film thickness of high polarity of (88%-cyanopropyl) aryl-polysiloxane capillary column. The oven was programmed with 70 ˚C for 1 minute then was increased by 2 ˚C/min to a final temperature of 120˚C for 1 minute. It shows that, among the samples, kerosene and diesel fuel have polar compounds due to their long elution in the high polar column.

Figure-3 shows the sensor response to exposure of gasoline in time domain. The noisy data - the output signal of F to V converter which interfered by high frequency oscillators - was improved by using a digital low-pass Butterworth filter with a 3-dB cut-off frequency of 0.2 Hz and a sampling rate of 10 Hz. The numerator and denumerator coefficients of the second-order recursive infinite impulse response filter is expressed by

$$y(n) = 0.0036\ x(n) + 0.0072\ x(n-1) + 0.0036\ x(n-2) + 1.8227\ y(n-1) - 0.8372\ y(n-2) \quad (2)$$

where, x and y are the input and output filter, respectively.

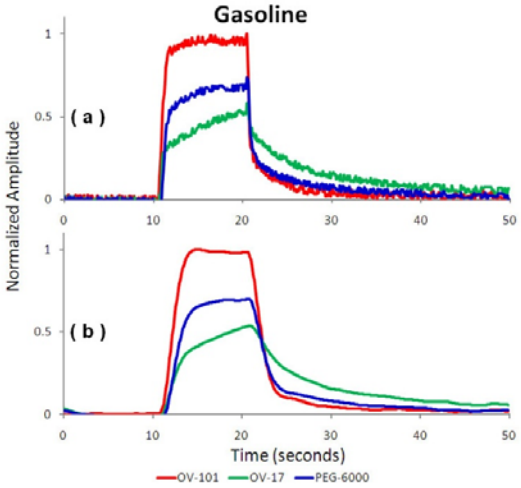

Figure-3. The sensor signal: (a) before and (b) after filtering.

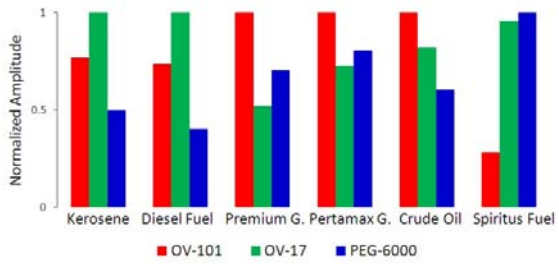

Figure-4. The response of the sensor array to fuel vapors.

Figure-4 shows the normalized patterns of the sensor array exposed to fuel vapors. Measurements of each sample were performed in 10 cycles. The average of relative standard deviation is 4.3%, which notably shows that the sensor array provides stable and reproducible signals.

According to Figure-2, due to the use of the polar column, the Premium and Pertamax gasoline have non polar compounds as indicated by the short duration with the peak amplitude at 2.045 and 2.091 minutes on the retention time. These compounds provide a strong interaction with non polar sensor material of OV-101 shown in Figure-4. On the other hand, the spiritus (methylated spirit) fuel - the ethanol denatured with 5% methanol- has a peak at 2.458 and 2.891 minutes, giving high responses to the sensor materials of OV-17 and PEG-6000. The hydrocarbons in crude oil are mostly non polar and mid polar compounds. Compared with other samples, kerosene and diesel oil have a low evaporation rate. The resulting minor number of compounds could be detected by the sensor array at room temperature with a slightly similar pattern for the two samples.

PCA is an effective and unsupervised pattern-recognition method that is often successfully used for investigating the performance of the electronic nose system [32]-[34]. This method is able to visualize the multi-dimensional data produced by n-sensors exposed to m-vapors onto lower dimension with a minimum loss of information. Figure-5 is the two dimensional plots of PCA obtained by the collection of maximum relative amplitudes of each sensor exposed to the set of fuel vapors during 10 cycles of measurement. The eigen-vector with the highest eigen-value is the first principle component containing the largest possible variance of the data set. The cumulative sum of the variances ordered by its eigen-value, from the highest to the lowest are:

63.5305
96.6781
100.0000

It shows that 97 % of the total variance within the data is contained in the first two principal components, which corresponds to the classification ability among the fuel vapors. In the case of gasoline, it is easy to separate two classes: Premium and Pertamax gasoline.

A neural network - another method of pattern recognition based on a biological neural network composition principle, with its parallel processing - has been used widely in electronic nose applications [34]-[38]. The network is formed in three layers, called the input layer, hidden layer, and output layer. In the feed forward network, the nodes or neurons between layers are fully connected with adjustable weights. Each neuron in the hidden and output layers also needs a bias weight.

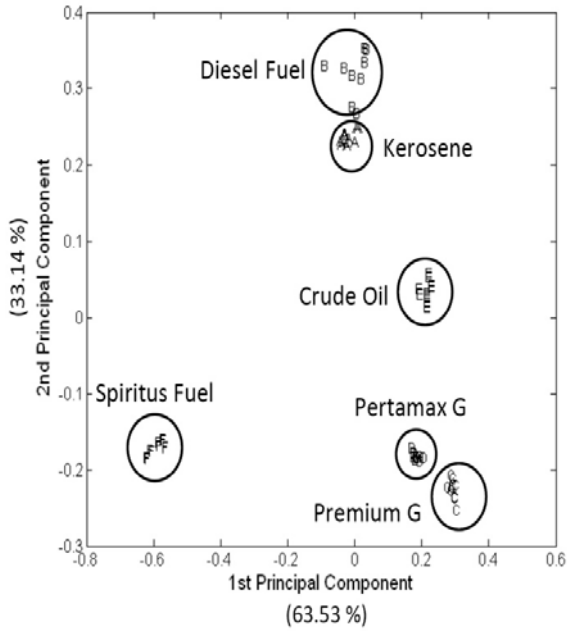

Figure-5. The scattering diagram of the fuel vapors plotted by PCA.

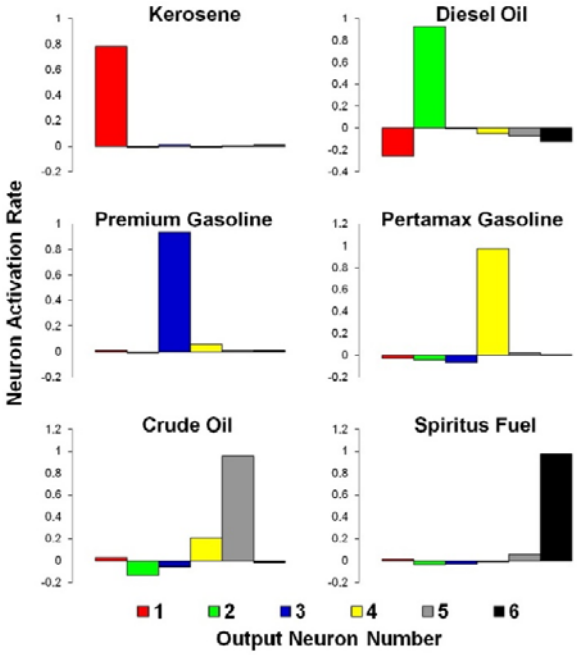

Figure-6. The output activation rates of the neural networks.

Back propagation is a common method of learning for the neural networks so as to minimize the objective function. In a supervised learning method, and a generalization of the delta rule, a dataset of the desired output (target) for many inputs, making up the learning set, is required. An error is calculated by comparing the target value with the output value. Gradient descent with momentum allows a network to respond not only to the local gradient, but also to recent trends in the error surface. The connection weights generated by the learning phase are saved as updated data. This step is repeated until the learning evaluation results are satisfied.

In this study, the input layer consisted of three nodes that correspond to the number of sensors. The hidden layer was composed of twenty neurons to accelerate and improve the convergence in the learning phase and the output layer that comprised of six neurons with respect to the number of fuel classes. All of the sensor values were normalized as real numbers between 0 and 1 by dividing them with the highest value. In the learning phase, the 30 data sets were fed into the network. Both the learning rate and moment constants were empirically determined to be 0.01. The network could be learned to classify each fuel vapor with the mean squared error of 1 % taking 7, 076 epochs. In the running phase, the other 30 data sets were fed into the feed forward network. The network can recognize all of fuel vapors with the identification rate of 100%. The activation rates of the output neurons are shown in Figure-6.

The next experiment conducted a measurement of blended fuel indicating adulteration rate. Premium gasoline and kerosene were mixed in volume by volume of six different proportions of 100:0, 80:20, 60:40, 40:60, 20:80 and 0:100. The final volume of the prepared fuel-adulterant mixture was 10 ml for each sample. Figure-7 shows the chromatograms of several gasoline mixtures. The isooctane compound having a peak at 3.346 minutes could be used as a marker of the blended fuel rate. The relative concentration of this compound tends to increase with increasing the percent of gasoline added (the 20%, 50% and 80% of gasoline correspond to the relative concentration of isooctane of 3.2%, 9.8% and 13.8%, respectively).

Measurements of each sample were performed in 10 cycles by the sensor array. The amplitude of a sensor must not depend on the sample concentration. Therefore, the concentration information was removed by dividing each sensor response with the others. The normalized sensor response (S) is expressed by

$$S_{i,k} = \frac{\Delta f_i}{\Delta f_k} \quad i \neq k \quad i,k = 1,2,...n \tag{3}$$

where, n is the number of sensors. In this case, we chose the positive correlation between the normalized sensor response and the adulteration rate.

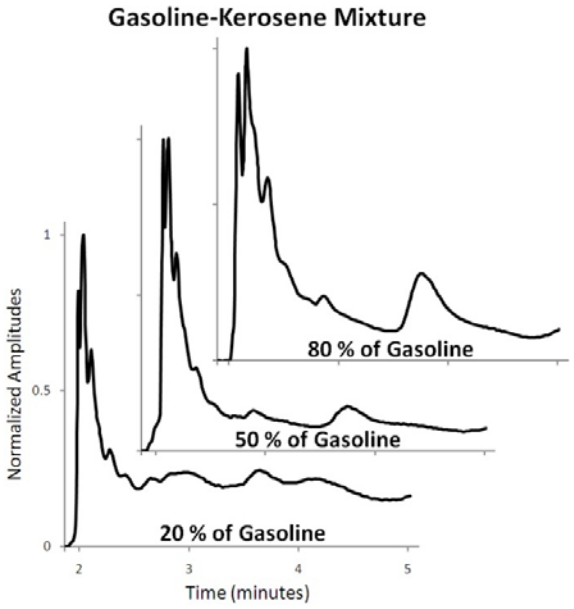

Figure-7. The chromatogram of the gasoline mixtures.

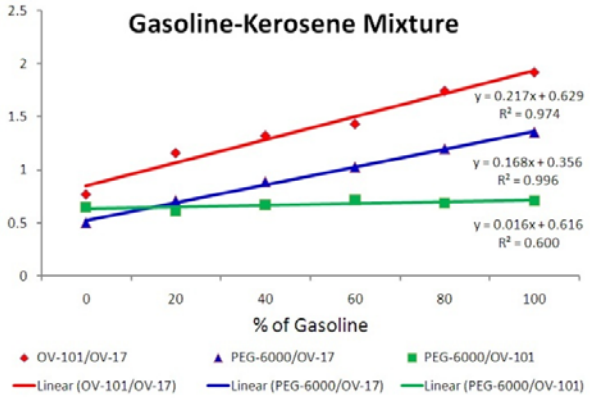

Figure-8. The sensor response to the variation of the gasoline mixture rate.

Figure-8 shows the sensitivity of sensor ratio to the variation of blended fuel rate. Although the ratio of OV-101/OV-17 has slightly higher sensitivity than that of the ratio of PEG-6000/OV-17, however, the latter has a higher coefficient of determination R^2 of 0.996 describing how well a regression line fits a set of fuel quality data.

CONCLUSIONS

Vapor sensor array composed of quartz crystals coated with different chemical materials could qualify fuels at room temperature. This sensor has been shown to resolve common fuels, including fuels of different classes (i.e., kerosene, diesel fuel, gasoline, crude oil, and spiritus) as well as within a particular class (i.e., Premium and Pertamax gasoline) with relative standard deviation is 4.3%. Principal component analysis indicates that 97% of the total variance within the data is contained in the first two principal components. The neural network can be taught to recognize all of the fuel vapors with the identification rate of 100 %. This sensor array could also determine the rate of fuel adulteration linearly with the determination coefficient of 0.996. These obtained results prove that this vapor sensor array can be used as a screening test for fuel quality. Instead of nitrogen for reference gas, the further study should be addressed to a low cost and portable dry air.

ACKNOWLEDGEMENT

This research was carried out with financial aid support from the Kementerian Riset, Teknologi dan Pendidikan Tinggi Republik Indonesia. The author would like to thank Associate Professor Takamichi Nakamoto, Department of Physical Electronics, Graduate School of Science and Engineering, Tokyo Institute of Technology, for providing the quartz sensors and ultrasonic atomizer facility.

REFERENCES

[1] Krzyzanowski M., Dibbert B. K. and Schneider J. 2005. Health effects of transport-related air pollution. Copenhagen, WHO Regional Office for Europe.

[2] Taylor E.T.; Nakai S. 2012. Monitoring the levels of toxic air pollutants in the ambient air of Freetown, Sierra Leone. African Journal of Environmental Science and Technology. 6, pp. 283-292.

[3] Salnikov V.G.; Karatayev M.A. 2011. The Impact of Air Pollution on Human Health-Focusing on the Rudnyi Altay Industrial Area. American Journal of Environmental Sciences. 7, pp. 286-294.

[4] Olmo N.R.S.; Saldiva P.H.N.; Braga A.L.F.; Lin C.A.; Santos U.P.; Pereira L.A.A. 2011. A review of low-level air pollution and adverse effects on human health: implications for epidemiological studies and public policy. Clinics. 66, pp. 681-690.

[5] Sinha S.N.; Shivgotra V.K. 2012. Environmental monitoring of adulterated gasoline with kerosene and their assessment at exhaust level. J. Environ. Biol. 33, pp. 729-734.

[6] Mattheou L.; Zannikos F.; Schinas P.; Karavalakis G.; Karonis D.; Stournas S. 2006. Impact of Using Adulterated Automotive Diesel on the Exhaust Emissions of A Stationary Diesel Engine. Global NEST Journal. 8, pp. 291-296.

[7] Obodeh O.; Akhere N.C. 2010. Experimental study on the effects of kerosene-doped gasoline on gasoline-powered engine performance characteristics. Journal of Petroleum and Gas Engineering. 1, pp. 37-40.

[8] Pauls R.E. 2011. A Review of Chromatographic Characterization Techniques for Biodiesel and Biodiesel Blends. Journal of Chromatographic Science. 49, pp. 384-396.

[9] Knothe G. 2001. Analytical Methods Used In the Production and Fuel Quality Assessment of Biodiesel. American Society of Agricultural Engineers. 44, pp. 193-200.

[10] Gerchman Y.; Schnitzer A.; Gal R.; Mirsky N.; Chinkov N. 2012. A simple rapid gas-chromatography flame-ionization-detector (GC-FID) method for the determination of ethanol from fermentation processes. African Journal of Biotechnology. 11, pp. 3612-3616.

[11] Balabin R.M.; Safieva R.Z. 2007. Capabilities of near infrared spectroscopy for the determination of petroleum macromolecule content in aromatic solutions. J. Near Infrared Spectrosc. 15, pp. 343-349.

[12] Ferrer C.A.B.; Mantilla L.Á.N. 2006. Rapid Characterization of Diesel Fuel by Infrared Spectroscopy. Ciencia Tecnologia y Futuro. 3, pp. 171-182.

[13] Binions R.; Afonja A.; Dungey S.; Lewis D.W.; Parkin I.P.; Williams D.E. 2011. Discrimination Effects in Zeolite Modified Metal Oxide Semiconductor Gas Sensors. IEEE Sensors Journal. 11, pp. 1145-1151.

[14] Neri G.; Bonavita A.; Micali G.; Donato N. 2010. Design and Development of a Breath Acetone MOS Sensor for Ketogenic Diets Control. IEEE Sensors Journal. 10, pp. 131-136.

[15] Szczurek A.; Maciejewska M.; Bodzoj L.; Wiercik B.F. 2010. A Concept of a Sensor System for Determining Composition of Organic Solvents. IEEE Sensors Journal. 10, pp. 924-933.

[16] Far A.B.; Flitti F.; Guo B.; Bermak A. 2009. A Bio-Inspired Pattern Recognition System for Tin-Oxide Gas Sensor Applications. IEEE Sensors Journal. 9, pp. 713-722.

[17] Partridge J.G.; Field M.R.; Sadek A.Z.; Zadeh K.K.; Plessis J.D.; Taylor M.B.; Atanacio A.; Prince K.E.; McCulloch D.G. 2009. Fabrication, Structural Characterization and Testing of a Nanostructured Tin Oxide Gas Sensor. IEEE Sensors Journal. 9, pp. 563-568.

[18] Ponzoni A.; Baratto C.; Bianchi S.; Comini E.; Ferroni M.; Pardo M.; Vezzoli M.; Vomiero A.; Faglia G.; Sberveglieri G. 2008. Metal Oxide Nanowire and Thin-Film-Based Gas Sensors for Chemical Warfare Simulants Detection. IEEE Sensors Journal. 8, pp. 735-742.

[19] Babaei F.H.; Golgoo S.M.H. 2008. Analyzing the Responses of a Thermally Modulated Gas Sensor Using a Linear System Identification Technique for Gas Diagnosis. IEEE Sensors Journal. 8, pp. 1837-1847.

[20] Chougule M.A.; Pawar S.G.; Patil S.L.; Raut B.T.; Godse P.R.; Sen S.; Patil V.B. 2011. Polypyrrole Thin Film: Room Temperature Ammonia Gas Sensor. IEEE Sensors Journal. 11, pp. 2137-2141.

[21] Iwaki T.; Covington J. A.; Gardner J.W. 2009. Identification of Different Vapors Using a Single Temperature Modulated Polymer Sensor With a Novel Signal Processing Technique. IEEE Sensors Journal. 9, pp. 314-328.

[22] Aguilar A.D.; Forzani E.S.; Nagahara L.A.; Amlani I.; Tsui R.; Tao N.J. 2008. A Breath Ammonia Sensor Based on Conducting Polymer Nanojunctions. IEEE Sensors Journal. 8, pp. 269-273.

[23] Meulendyk B.J.; Wheeler M.C.; Cunha M.P. 2011. Hydrogen Fluoride Gas Detection Mechanism on Quartz Using SAW Sensors. IEEE Sensors Journal. 11, pp. 1768-1775.

[24] Jha S.K.; Yadava R.D.S. 2009. Preprocessing of SAW Sensor Array Data and Pattern Recognition. IEEE Sensors Journal. 9, pp. 1202-1208.

[25] Wen C.; Zhu C.; Ju Y.; Xu H.; Qiu Y. 2009. A Novel Dual Track SAW Gas Sensor Using Three-IDT and Two-MSC. IEEE Sensors Journal. 9, pp. 2010-2015.

[26] Liu J.; Wang W.; Li S.; Liu M.; He S. 2011. Advances in SAW Gas Sensors Based on the Condensate-Adsorption Effect. Sensors. 11, pp. 11871-11884.

[27] Saraoglu H.M.; Kocan M. 2010. Determination of Blood Glucose Level-Based Breath Analysis by a Quartz Crystal Microbalance Sensor Array. IEEE Sensors Journal. 10, pp. 104-109.

[28] Pais V.F.; Oliveira J.A.B.P.; Gomes M.T.S.R. 2012. An Electronic Nose Based on Coated Piezoelectric Quartz Crystals to Certify Ewes' Cheese and to Discriminate between Cheese Varieties. Sensors. 12, pp. 1422-1436.

[29] Selyanchyn R.; Korposh S.; Wakamatsu S.; Lee S.W. 2011. Respiratory Monitoring by Porphyrin Modified Quartz Crystal Microbalance Sensors. Sensors. 11, pp. 1177-1191.

[30] Rivai M.; Purwanto J.; Juwono H.; Sujono H.A. 2011. Electronic Nose using Gas Chromatography Column and Quartz Crystal Microbalance, Telkomnika. 9, pp. 319-326.

[31] Aguirre S.M.; Nakamoto T.; Moriizumi T. 2005. Study of deposition of gas sensing films on quartz crystal microbalance using an ultrasonic atomizer. Sensors and Actuators B. 105, pp. 144-149.

[32] Tian X.Y.; Cai Q.; Zhang Y.M. 2012. Rapid Classification of Hairtail Fish and Pork Freshness Using an Electronic Nose Based on the PCA Method. Sensors. 12, pp. 260-277.

[33] Tian F.; Li H.; Zhang L.; Liu S.; Ye Q.; Hu B.; Xiao B. 2012. A Denoising Method Based on PCA and ICA in Electronic Nose for Gases Quantication. Journal of Computational Information Systems 8, pp. 5005-5015.

[34] Chen C.C.; Shih J.S. 2008. Multi-Channel Piezoelectric Quartz Crystal Sensor with Principal Component Analysis and Back-Propagation Neural Network for Organic Pollutants from Petrochemical Plants. Journal of the Chinese Chemical Society. 55, pp. 979-993.

[35] Kumar R.; Das R.R.; Mishra V.N.; Dwivedi R. 2009. A Radial Basis Function Neural Network Classifier for the Discrimination of Individual Odor Using Responses of Thick-Film Tin-Oxide Sensors. IEEE Sensors Journal. 9, pp.1254-1261.

[36] Men H.; Liu H.; Pan Y.; Wang L.; Zhang H. 2011. Electronic Nose Based on an Optimized Competition Neural Network. Sensors, 11, pp.5005-5019.

[37] Fu J.; Li G.; Qin Y.; Freeman W.J. 2007. A pattern recognition method for electronic noses based on an olfactory neural network. Sensors and Actuators B. 125, pp. 489-497.

[38] Kim E.G.; Lee S.; Kim J.H.; Kim C.; Byun Y.T.; Kim H.S.; Lee T. 2012. Pattern Recognition for Selective Odor Detection with Gas Sensor Arrays. Sensors. 12, pp. 16262-16273.